CHAPTER 4

NUMERICAL EXAMPLES AND RESULT VALIDATION

4.1 Programming structures

The structure of the program to solve the band gap characteristic using FEM for such lossless, isotropic, and non-magnetic 2D PCs arranged as in Figure 4.1. From the parameter input step, due to the assumption that the analyzed system is lossless, isotropic and consists of non-magnetic materials, the relative permittivity becomes real, scalar, and independent with the frequency while the relative permeability remains unity. Here the relative permittivity of the rod vary such that $\varepsilon_{r,\text{rod}}$=8.9 (equal to which of alumina crystal) for analyzing the square lattice PCs and $\varepsilon_{r,\text{rod}}$=11.4 (equal to which of GaAs [23]) for analyzing the triangular lattice PCs while maintaining $\varepsilon_{r,\text{medium}}$=1 (equal to which of air medium). These are known that for the same lattice system, the higher the difference between the two dielectric constants, the larger band gap is obtained [1,4,23]. The length of the periodicity a is the physical parameter of PCs on the order of the wavelength of the relevant optical wave for the PCs that can lead the system into nano-scale length devices to support the nanotechnology world. Another contribution of a is to define the filling factor or the volume fraction which is related to the radius of the rod r such that $r=C.a$ where C is a constant and here C = 0.2 for both square and triangular lattice PCs. Other parameter inputs are wave vectors, which are taken from the irreducible Brillouin zone (the wave vector zone) and sampled as shown in Figure 2.7.

Data from mesh generator are exported to the main FEM program to get the information about the numbers and coordinates of nodes as well as elements. The format of the data must be arranged properly according to how the program reads the data. The data of boundary nodes are important since they are used to assign the boundary condition i.e. PBC where the wave vector inputs are assigned. Therefore, the parallelism of the position of nodes on mirroring edges must be maintained.

When the PBC are imposed, the generated matrices constructing the eigensystem are modified. The matrices before are complex, sparse, and symmetric due to the FEM formulations. After imposing the PBC, the matrices become sparse, complex, and non-symmetric. The un-symmetric matrices occur because imposing the PBC modify the eigen-matrices by removing columns and rows containing the periodic nodes, which are dependent to other nodes. To solve the eigenvalues, function *eig*() in MATLAB is used to find the solutions.

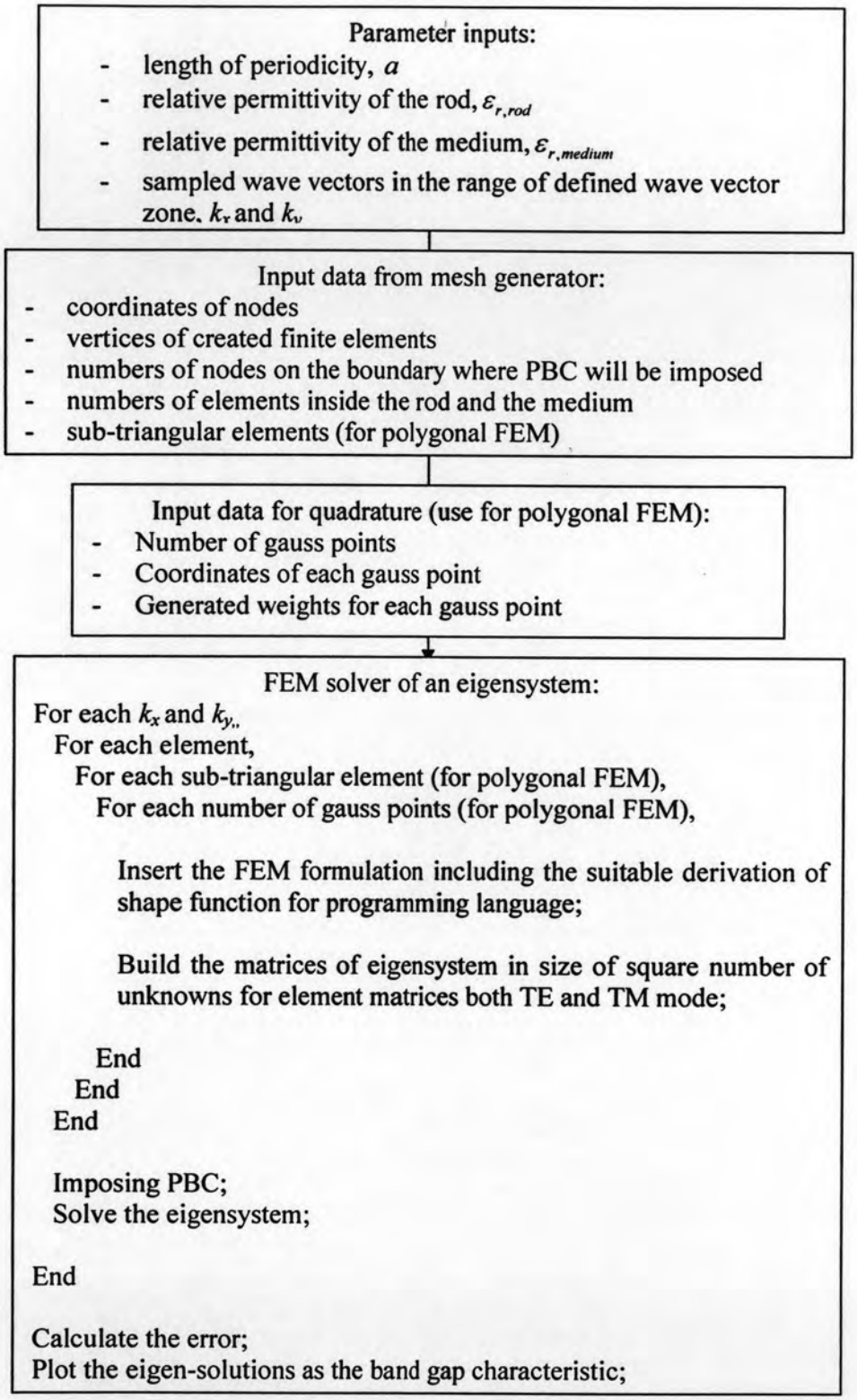

Figure 4.1 Programming structures of FEM to solve the band gap characteristic.

4.2 Validation of the results

The results from the proposed method are validated using the procedure shown in Figure 4.2 below.

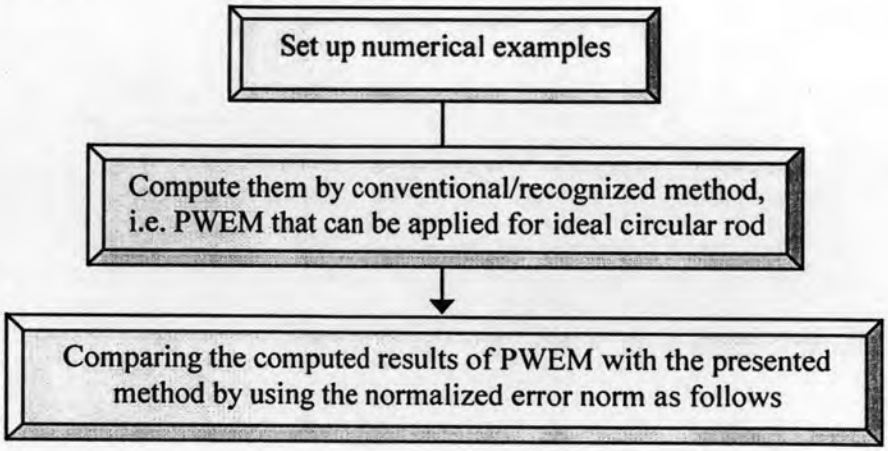

Figure 4.2 A validation procedure for the results from the proposed method

The numerical examples set up here are square lattice and triangular lattice PCs in case of rods embedded in air medium where the dielectric constants for the rods are 8.9 and 11.4, respectively for each lattice. The ratio between the radius of the rod and the lattice constant is 0.2 for both lattices. The solutions for band gap characteristics obtained from the proposed method are validated with which from the conventional/recognized method as the reference solutions. The reference solutions are calculated using PWE method which is a semi-analytical method applied normally for ideal circular rod. The difference of both approximate and reference solutions is measured to see how big the error and how far the solution to be converged.

This validation is performed in calculation of error values for both numerical methods using a formulation of error L_2 norm as in (4.1).

$$\left\|u-\bar{u}\right\|_{L^2(\Omega)} = \sqrt{\int_{\Omega}(u-\bar{u})^2 d\Omega} \tag{4.1}$$

The L_2 norm is employed for error estimations. A norm is a real valued function that provides a measure of how well a given approximate solutions $\bar{u}$ relative to the reference solutions u where here both $\bar{u}$ and u are in vector forms. When the norm is applied to discrete number of solutions, the integral functions become summation of all the values as shown in (4.2) in the same space which is known as the Euclidean space.

$$\left\|u-\bar{u}\right\|_{L^2(\Omega)} = \sqrt{\sum_{i=1}^{N}(u-\bar{u})^2} \tag{4.2}$$

This norm possesses a natural norm defined as in (4.3) in continuous forms.

$$\left\|u\right\| = \sqrt{\langle u,u\rangle} = \sqrt{\int_{\Omega}u^2 d\Omega} \tag{4.3}$$

Equation (4.1) accumulates the difference between the approximate unknown values and the reference solutions so that the total errors can be evaluated by taking the integral function over the domain of calculation. The error levels are evaluated by taking the error norm in (4.1) and normalized it with the natural norm in (4.3) as in (4.4)

$$\text{Normalized error norm} = \frac{\|u-\bar{u}\|_{L^2(\Omega)}}{\|u\|_{L^2(\Omega)}} \tag{4.4}$$

The error term here is the difference between the approximate solutions and the reference ones. It can be used to indicate how far the available approximation system can reach the reference solutions. Smaller values of the errors are assumed to give the higher accuracy. Approximation process such as in FEM is a kind of adaptive process where the process will be repeated until the errors are minimized or until certain desired condition is accomplished by changing the properties of the FEM such as the number of nodes or the number of elements. The certain condition in this problem is more subjected to achieve the range of the band gap accurately.

The difference values of both solutions, i.e. $(u-\bar{u})$, can be either negative or positive so it will be more stable to represent them in their absolute values or some normalized measure of them. It involves the integral of the square of the argument. The purpose in doing the numerical analysis is to minimize the error in the solution i.e. $(u-\bar{u})$ and L_2 norm is common to be employed to estimate the error [13, 18, 33]. The relative error is defined as in (4.4) which relate the error norm to the norm of the reference solutions. Sometimes, the relative error norm is represented in percentage value, which needs to be multiplied by 100 %.

The reference solutions used here come from the PWEM as used in [7]. The solutions from PWEM are obtained by running MPB software, which is downloaded freely. The resolution is set to be 128 x 128. Figure 4.3 shows the results from PWEM for square and triangular lattice PCs where a dielectric rod is surrounded by an air medium. In the square lattice PC, the relative permittivity (or dielectric constant) of the rod, ε_r, is equal to 8.9 as which for alumina while in the triangular lattice PC, ε_r is chosen as which of a glass i.e. 11.4 for variation.

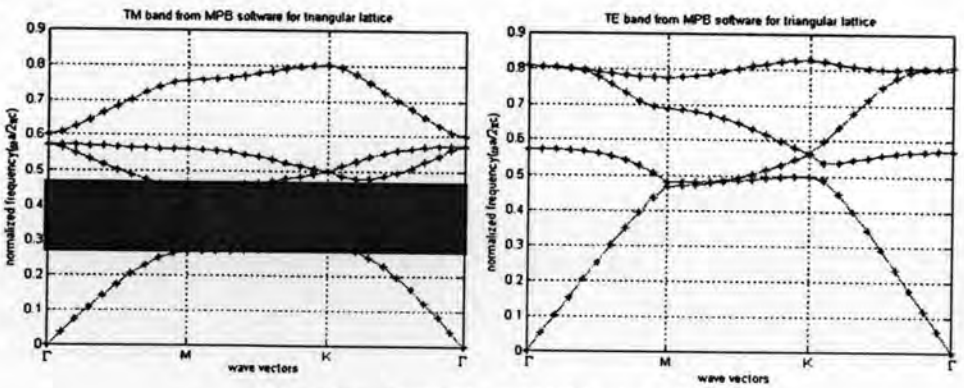

(a) a dielectric rod with ε_r=11.4 in air medium

Figure 4.3 References of band gap characteristic from PWE for (a) triangular and (b) square lattice PCs.

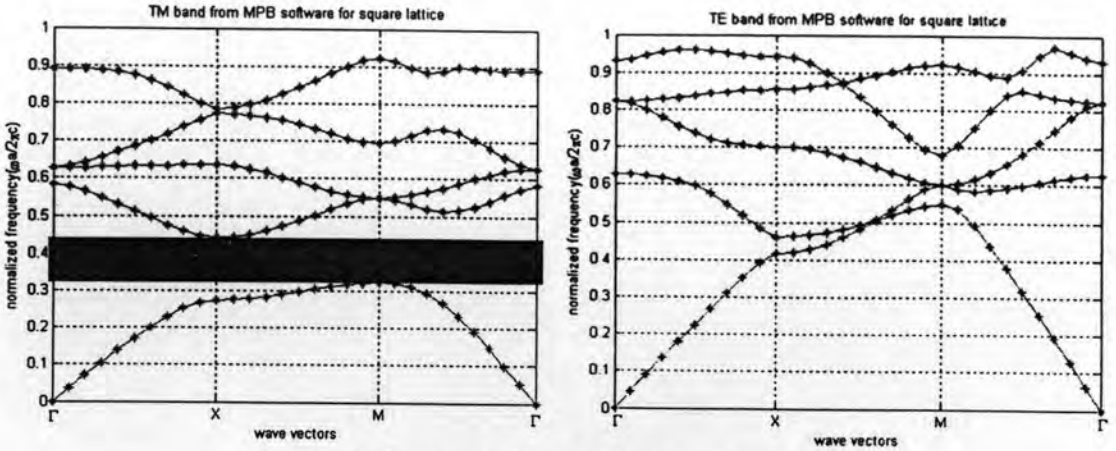

(b) a dielectric rod with ε_r=8.9 in air medium

Figure 4.3 References of band gap characteristic from PWE for (a) triangular and (b) square lattice PCs (cont.)

4.3 Numerical efficiency of polygonal FEM results

Some numerical results are shown in this chapter. The errors of the results are calculated in order to analyze and to see the performance and the efficiency of the method. The terminology of numerical efficiency will provide the related information about how efficient the polygonal method is to calculate the band gap characteristic compared with the linear triangular FEM. Both results from linear triangular FEM and polygonal FEM are validated using PWE. The behavior of the system will be presented and the relationship between the patterns of mesh of polygonal elements will be shown for n=3, n>3, and combination of n≥3. At this section, the performance of the proposed method, i.e. polygonal FEM, is investigated. The method is also applied to a square and a triangular lattice unit cells. The comparison of the performance of different n-gons used in a designed mesh is presented for n=3, 4, 5, and greater than 5. Since increasing the number of n in the element will increase the order of the element by using Wachspress shape function, an improvement in accuracy is expected. The flexibility of the arbitrary polygons used in the designed mesh is shown by the performance of the mesh used in FEM to approximate the solutions.

4.3.1 Square lattice PC

The result of polygonal FEM for the square lattice PC shows an agreement to the reference solution. The polygonal mesh used to approximate the solution is shown in Figure 4.4a while the result band gap characteristics are given in Figure 4.4b.

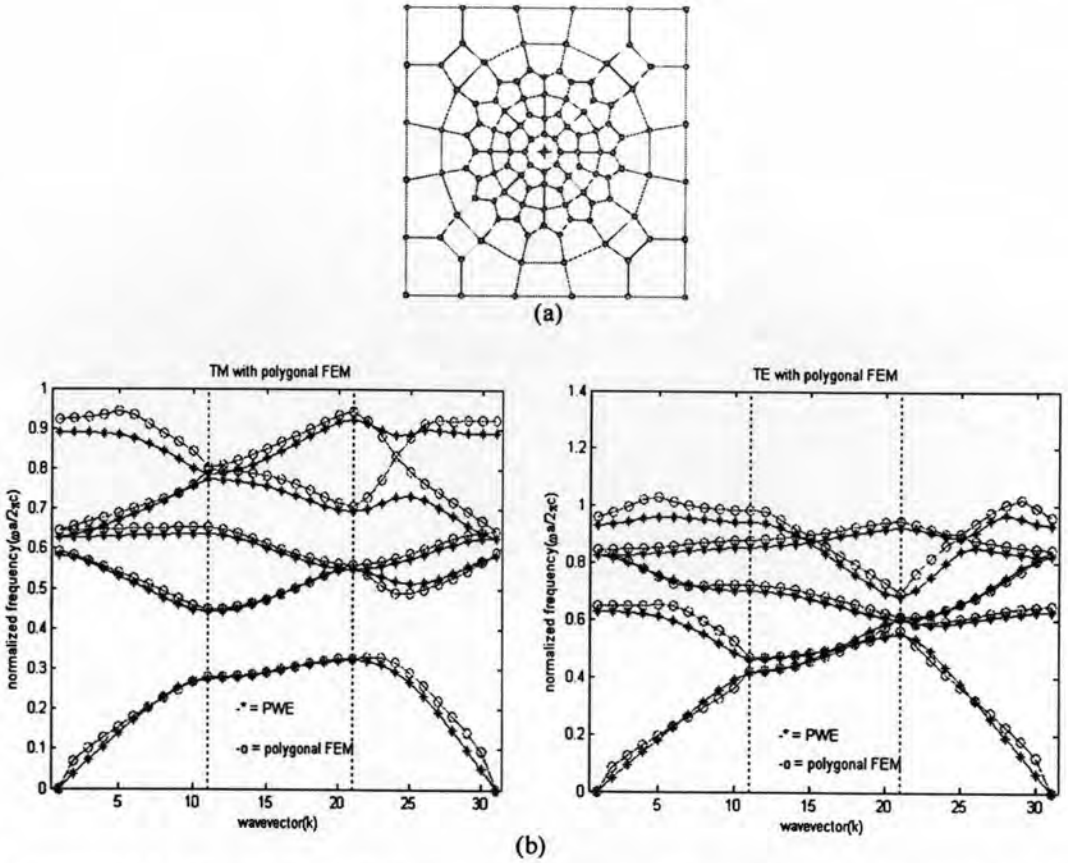

Figure 4.4 (a) A polygonal mesh with dominant n=5 elements and (b) result band gap characteristic for TM and TE modes.

The results show the agreement of the shape of the curves for both TM and TE modes. Some parts look not converged mainly in the higher frequency bands due to the higher dynamism of the bands. The approximate solutions are plotted in red curves while the reference solutions from PWE are given with the blue ones. The available band gap over the defined wave vectors looks approximated sufficiently. In this case, the mesh is sufficient in order to approximate the frequency band gap since this is the main property of such band gap characteristics.

The polygonal mesh consists of different n-gonal elements with n=5 elements are dominant. Generating higher order elements will face a slight difficulty since it would not be easy to maintain the conformity among the elements especially on the boundary areas. The uniformity of the element type would break when the n>4 elements are used. Therefore, the ability to build meshes from various types of elements must be established. Applying the Wachspress shape function supports that requirement. This condition also proves the greater flexibility of the polygonal mesh using Wachspress shape function on the arbitrary convex polygonal mesh.

4.3.2 Triangular lattice PC

The polygonal FEM is also applied to another example case, i.e. triangular lattice PC. The mesh and its result band gap characteristics are shown in Figure 4.5.

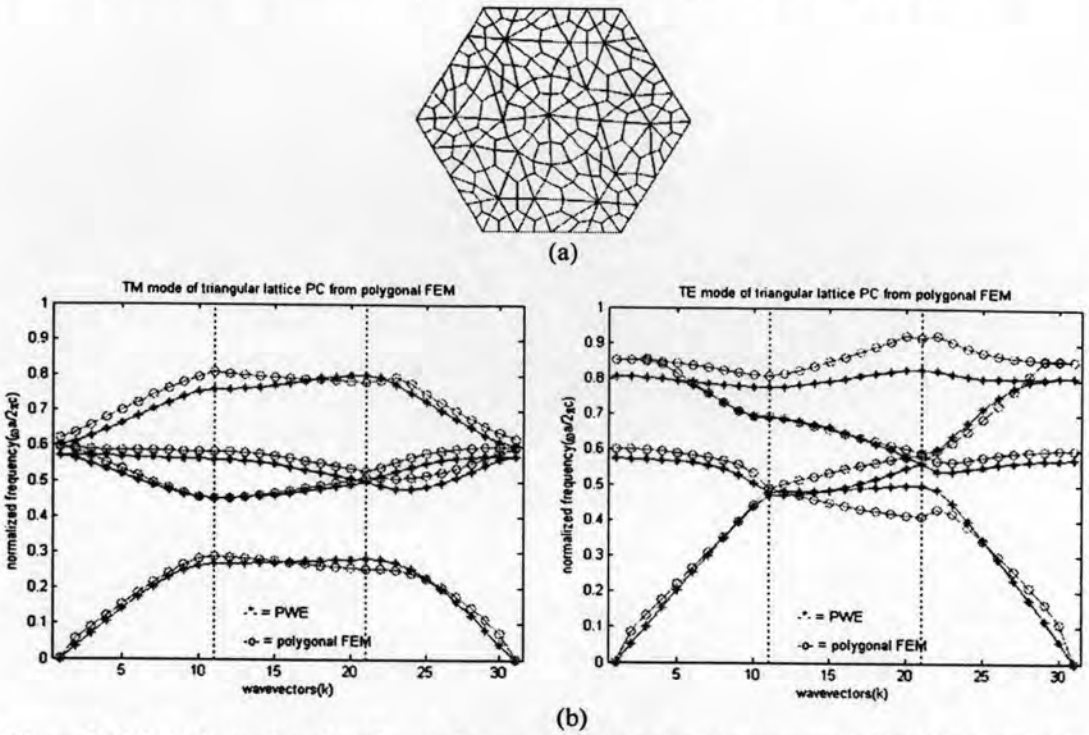

(a)

(b)

Figure 4.5 (a) a polygonal mesh with n=4 elements and (b) band gap characteristic for TM and TE modes.

Comparing the band gap characteristic of the approximate and reference solutions shows good agreements for TM mode. In TE mode, a discrepancy occurs in the middle area of the wave vectors, i.e. area M-K. An improper boundary condition applied may cause this condition. Since there is no band gap available, the discrepancy in TE mode solution may not affect the function in practical.

4.4 The effect of higher order elements in polygonal FEM

4.4.1 Square lattice unit cell

The case of square lattice, the generated meshes are shown in Figure 4.6 follows.

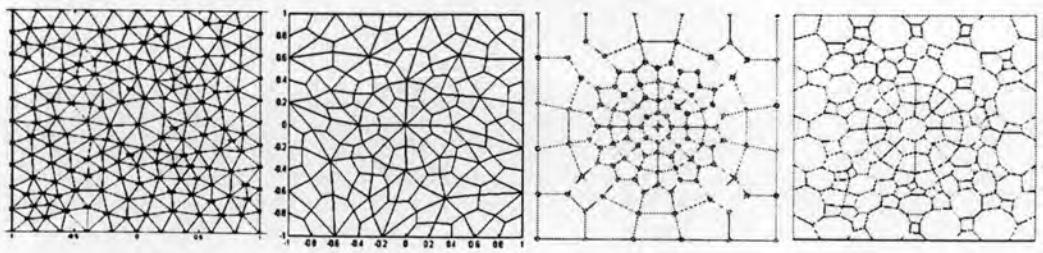

(a) (b) (c) (d)

Figure 4.6 Generated polygonal meshes with (a) n=3, (b) n=4, (c) n=5 dominant, and (d) n>5 dominant

Table 4.1 Specification of the polygonal meshes and their average error on a square lattice unit cell

Mesh Type	Triangular Mesh I	Test Mesh I (n=4)	Test Mesh II (n=5 dominant)	Test Mesh III (n>5 dominant)
Number of nodes	186	177	116	263
Number of elements	330	156	77	145
Av. Error TM mode	0.04173	0.04070	0.03877	0.03143
Av. Error TE mode	0.04137	0.04062	0.03884	0.03321

Test Mesh I is generated directly by using the available mesh generator tools for n=4 (rectangular elements) while the Test Mesh II is created manually with the aids of the tools. Test Mesh I has a greater number of unknowns than which from the Test Mesh II. However, the Test Mesh II provides greater accuracy for both TM and TE modes. The Test Mesh II with higher n-gons and less number of unknown already proved to give the better results to which of Test Mesh I with lower n-gons and greater number of unknowns. These results are compared to which from the previous linear triangular elements and they prove to have better accuracies and less number of unknowns. It is confirmed with the derivation of the interpolation function in Chapter 3 that the higher n-gons provide the higher interpolation functions.

The Test Mesh I is all rectangular elements which employees single type of polygons while the Test Mesh II is a combination of several types of n-gons that prove to give better accuracy. This condition indicates that the conformity of the arbitrary polygonal elements in the designed mesh is held by using the Wachspress shape function since this interpolation function is linear on the boundary of the elements but it becomes higher order inside the elements so that the higher accuracy can be obtained. Applying the polygonal FEM using Wachspress shape functions yields higher order of elements as well as the interpolation function and also provides the higher flexibility in choosing elements for the mesh compared with which of linear triangular FEM. Another significant preference shown in Figure 4.7 is the comparison of the employed number of elements. The efficiency of the higher n-gons in a polygonal mesh is high compared to the lower n-gonal elements.

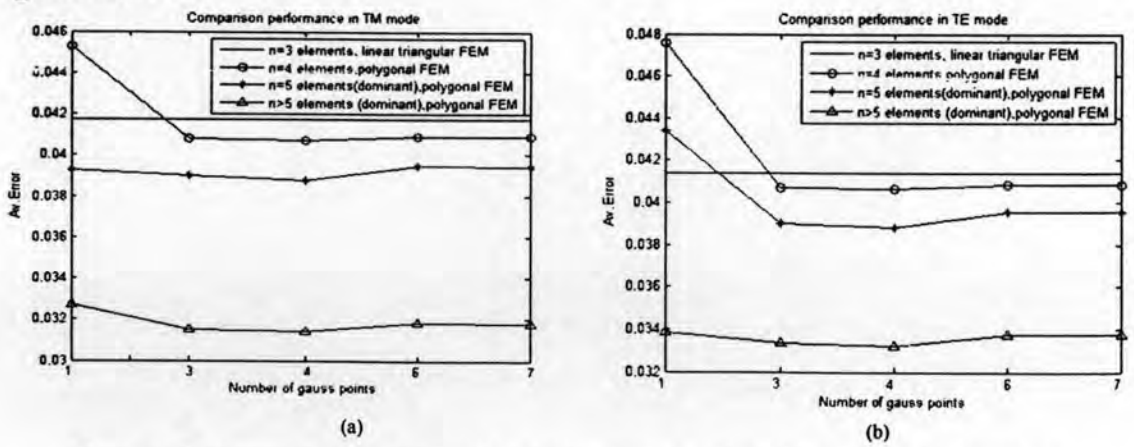

Figure 4.7 The comparison of accuracy from mesh with n=3, n=4, and dominant n=5 elements for (a) TM mode and (b) TE mode.

The purpose of these designs is to show the accuracy of the polygonal FEM using the Wachspress shape functions compared with which of the linear triangular FEM. Since the Wachspress shape functions become similar to the common area coordinates in linear triangular FEM when they are applied to n=3 elements (linear triangular elements), the comparison results also tells the performances of each type of polygonal elements in the FEM meshes. The comparison graph is shown in Figure 4.7.

The figure proves that for such types of meshes, the higher n-gonal meshes provide the better accuracy for the average error. The result from linear triangular FEM is shown to give the comparative results although there is no relationship to the variation of the number of gauss points. Among the polygonal FEM, the optimum number of gauss points here is 4 where this value gives the lowest error as presented in the Figure 4.7. The positions and the weights of these points are given in Chapter 3. Both TM and TE modes show the similar behaviors of the accuracy performance. The errors calculated here are which of normalized error norms explained in the beginning of this chapter. All these calculations are done using 31 samples of k's since increasing the number of sample wave vectors would not give much improvement in accuracy. Moreover, less number of sample wave vectors will make the calculation time is reducing. The band gap characteristics are shown in the Figure 4.8 and Figure 4.9 for which of both Test Mesh I and Test Mesh II, respectively.

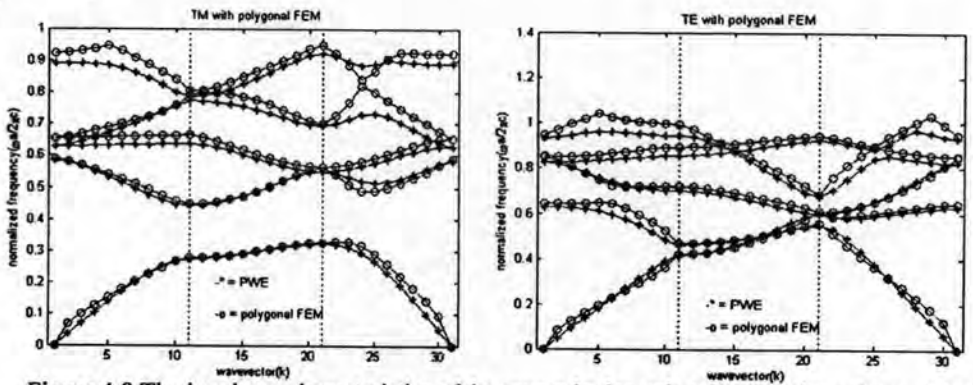

Figure 4.8 The band gap characteristics of the square lattice unit cell using the polygonal FEM employed Test Mesh I

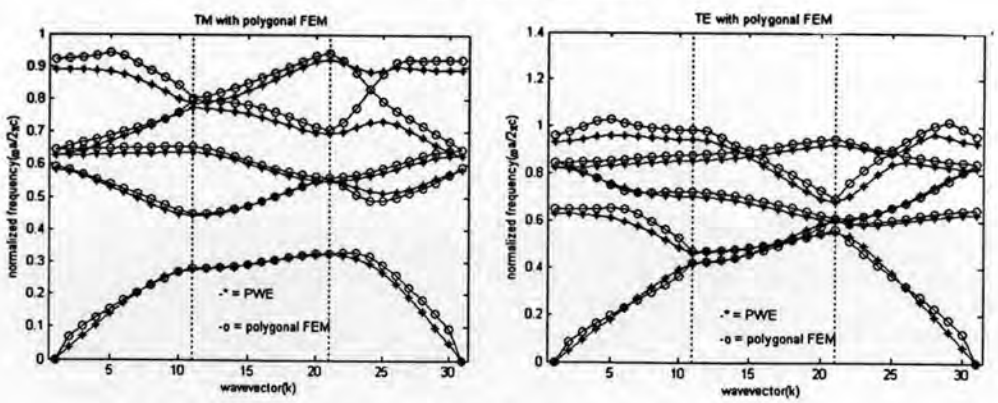

Figure 4.9 The band gap characteristics of the square lattice unit cell using the polygonal FEM employed Test Mesh II

The results of the band gap characteristics look similar for both of Test Mesh I and Test Mesh II. However, the accuracy in terms of calculation errors from Test Mesh I is higher than which from Test Mesh II as given before. Since the important thing of this frequency map is the band gap, Table 4.2 gives the estimation error of the available band gap for both polygonal meshes compared with that from linear triangular Mesh I.

From Table 4.2, the Test Mesh I provides lower error of the band gap ranges than that from Test Mesh II although the last polygonal mesh gives the higher average accuracy for the band gap characteristic and the errors of both lower and upper edges of the gap yield almost the same accuracy for each of them. However, these errors of band gap ranges from the higher *n*-gonal elements are still better than the linear triangular elements.

Table 4.2 Comparison errors of band gap ranges in TM mode of a square lattice unit cell for both polygonal FEM and the linear triangular FEM.

Mesh	Error of lower frequency of the gap (%)	Error of upper frequency of the gap (%)	Error of band gap ranges (%)	Ratio of the predicted width of band gap with PWEM
Triangular Mesh 1, n=3	1.79765	1.17484	0.49746	99.5%
Test Mesh 1, n=4	1.71973	1.27276	0.07257	100,07%
Test Mesh II, n=5	1.67237	1.28678	0.25142	100,25%
Test Mesh III, n>5	1.45012	0.61090	1.64249	98,35%

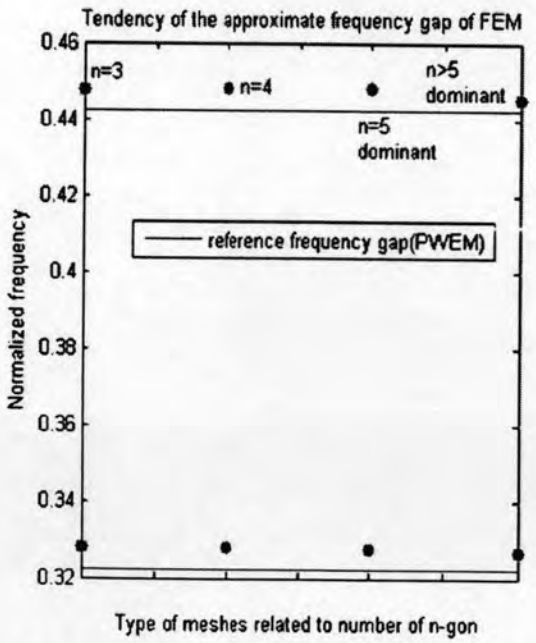

Figure 4.10 Tendency of the approximate frequency band gap relative to employed *n*-gonal elements

The tendency of error of lower frequency of the gap is reducing with the increasing the order of the used elements while the one from upper frequency increases a little bit but after that decrease quite significantly. Finally, the approximate solutions of the n>5 dominant mesh yield the closest values to the reference solutions although the error range of the obtained band gap increases. This condition occurs because the value of the upper frequency gap converges faster that the lower frequency so that the range of the approximate band gap is reducing and the error increases as shown in Figure 4.10. When the width of the obtained frequency band gap is compared to the width of reference frequency band gap, the results from this method yield ratios of around 100%.

Based on these results, there is a new comparative result from the work of Ming-Chieh Lin and Ruei Fu Jao in [35] where they used the FEM with 6-node triangular FEM with 5th-order basis function in order to give high accuracy computation compared with PWEM as well. Their results provided that error lower frequency gap is 0.26% and error upper frequency gap is 2.6%. The predicted width of the band gap shows 65% discrepancy from PWEM. In this case, the effort to increase the accuracy is more tedius where a complicated derivation for the basis function must be taken and the large number of unknowns in higher order triangular elements. Hence, the proposed method here looks better in the derivation of the shape function and in the number of unknowns since the predicted widths of the band gaps here give around 100% of their ratio.

4.4.2 Triangular lattice case

Beside applying the polygonal FEM to the square lattice unit cell, this polygonal FEM is also applied in the triangular lattice unit cell. On that hexagonal domain, the discretization is done by using arbitrary polygonal elements. The first polygonal mesh is created by combining some triangles together into a polygonal element as shown in Figure 4.11.

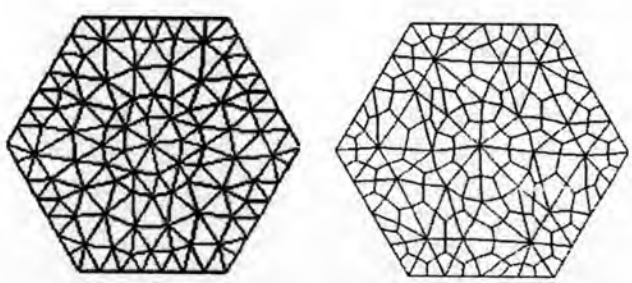

Figure 4.11 Polygonal meshes on triangular lattice unit cell by (a) converting some triangular elements into a polygonal element called Mesh I and (b) Mesh II created by the available mesh generator tool.

To continue the investigation, another polygonal mesh on this hexagonal domain is built. The mesh generator tool do this directly by using rectangular elements and creates Mesh II shown Figure 4.11. The specification of the built meshes is given by Table 4.3.

Table 4.3 Specification of mesh for polygonal FEM of a triangular lattice unit cell and calculation error.

Mesh Type	Mesh I (n=3)	Mesh II (n=4)
Number of nodes	113	99
Number of elements	182	78
Av. Error TM mode	0.05154	0.04319
Av. Error TE mode	0.07296	0.06610

With less number of unknowns (nodes) and less number of elements, the Mesh II provides lower error which means that the method performs higher accuracy than which of Mesh I as shown in table 4.3. This early results prove the higher efficiency of the polygonal FEM than the linear triangular FEM in terms of number of nodes and number of elements. The results of the band gap characteristics are shown in Figure 4.12.

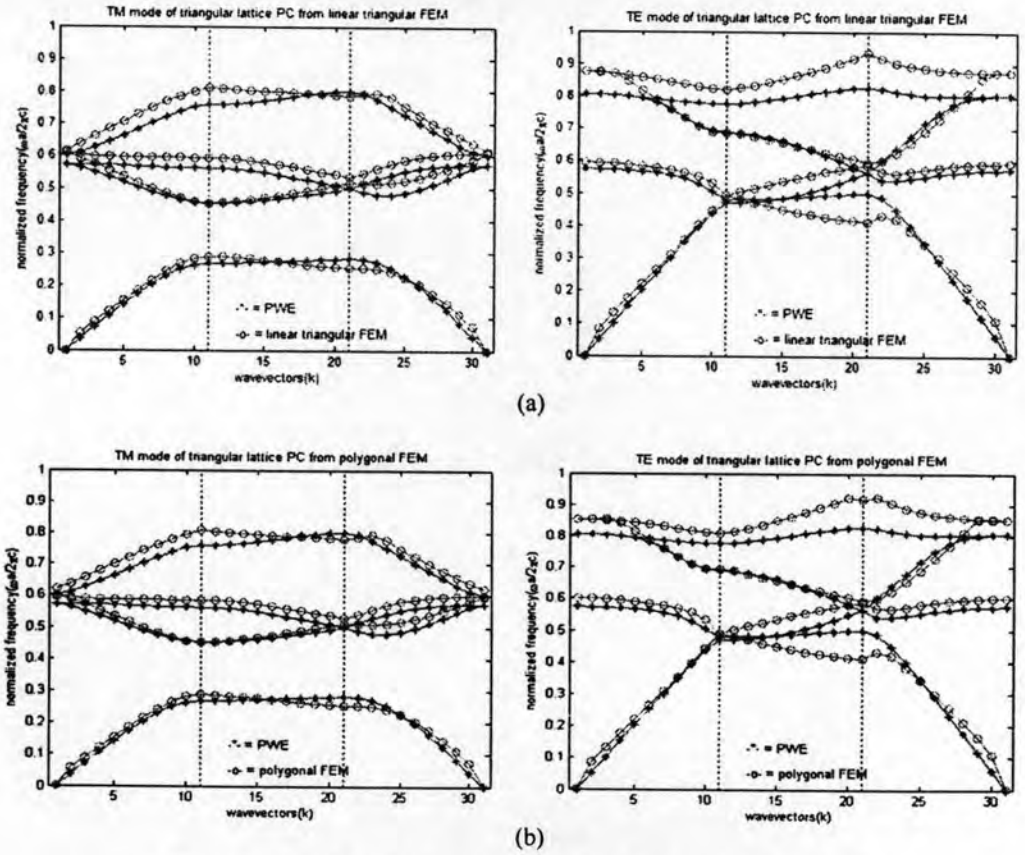

Figure 4.12 Band gap characteristics of the triangular lattice PC using (a) linear triangular and (b) polygonal FEM.

The obtained error of the band gap is given in Table 4.4. The results show that there is a slightly improvement of the accuracy for the values of both lower and upper edges of the gap but this condition undesirably increase the error of the band gap range.

Table 4.4 Comparison errors of band gap ranges in TM mode of a triangular lattice unit cell for both polygonal FEM and the linear triangular FEM.

Mesh	Error of lower frequency of the gap (%)	Error of upper frequency of the gap (%)	Error of band gap ranges (%)
Triangular Mesh I	2.63994	0.27965	3.60427
Test Mesh 1	2.09762	0.22521	4.04749

However, the result from polygonal FEM indicates to give better accuracy than which of the linear triangular FEM does as shown in Figure 4.13.

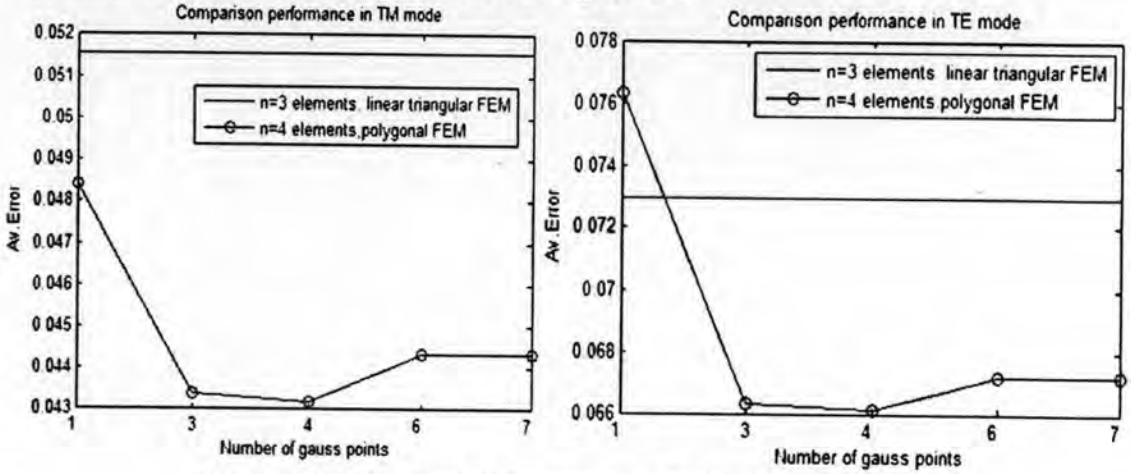

Figure 4.13 Performances of linear triangular FEM and polygonal FEM with variation numbers of gauss points for TM and TE modes

As obtained in the previous results of the square lattice PC, the optimum number of gauss points using in the polygonal FEM can be 3 or 4 points where the lowest error is obtained for such designed polygonal mesh.

4.5 Hybrid polygonal FEM

The polygonal FEM applied in the square lattice unit cell employees finite elements whose $n>3$ while in the triangular lattice unit cell, the polygonal FEM employed elements whose $n\geq 3$. The combination between the linear and the higher order elements is investigated and it is called as hybrid polygonal FEM. The hybrid polygonal FEM is mixed elements of linear and higher order ones as well as the combination of linear and higher order polynomial shape functions. The used designed meshes are shown in Figure 4.14 with their specifications are given in Table 4.5.

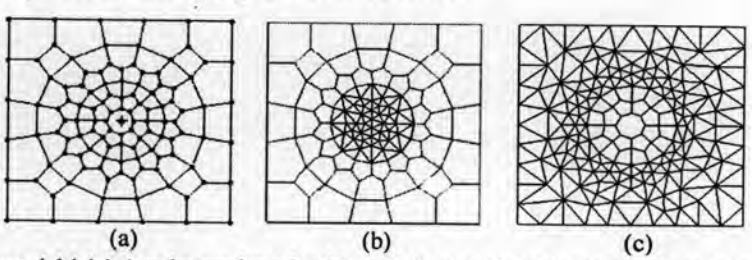

Figure 4.14 (a) A polygonal mesh with n>3, (b)-(c) Hybrid polygonal meshes I-II

Table 4.5 Specification of mesh for polygonal FEM of a square lattice unit cell and calculation error.

Mesh Type	Polygonal Mesh	Hybrid Mesh I	Hybrid Mesh II
Number of nodes	116	128	180
Number of elements	77	134	281
Av. Error TM mode	0.03877	0.03781	0.03879
Av. Error TE mode	0.03884	0.03768	0.03837

The FEM calculations show that the Hybrid Mesh I indicates to give better accuracy than the original polygonal mesh and the Hybrid Mesh II. The number of triangles either in the rod (Hybrid Mesh I) or in the medium (Hybrid Mesh II) equal to the number of sub-triangles used in the numerical integration of the original polygonal mesh such that those accuracies are obtained. This Hybrid Mesh I and II break the efficiency in terms of number of nodes and elements. However, these kinds of meshes show the conformity between the linear and the higher order property of both elements and polynomial interpolation functions.

The increased accuracy is related to the behavior of the system. In Hybrid Mesh I, the polygonal elements are placed in the air medium of the unit cell and the linear triangular elements are assigned on the dielectric rod. Over such a unit cell, the electric fields automatically are more concentrated in the higher dielectric rod rather than in the air medium. According to the TM mode solution from the wave equations in (2.55)-(2.56), the higher the dielectric constant of the material, the lower frequency of the fields are obtained. The lower frequency will make the behavior of the systems remain constant while the higher frequency will give a dynamic behavior to that system. The dynamism of the system can be noticed from the fluctuating modes that exist on that region. This condition is held for the square lattice unit cell where the existing modes are shown in Appendix A together with which of the triangular lattice unit cell.

These results show that for the domain which is less dynamic (non-fluctuating), the linear triangular elements are suitable enough for meshing on that domain while for the more dynamic (fluctuating) domain, the higher order elements are recommended to be assigned such as those polygonal elements.

In contradiction, although the number of nodes and elements in Hybrid Mesh II are larger than which are in Hybrid Mesh I, the obtained accuracies are lower. The larger number of linear elements on that fluctuating domain cannot perform as good as the polygonal elements to approximate the solutions.

Table 4.5 shows the error of the band gap calculation where both hybrid meshes yield the same accuracy of the band gap ranges. The Hybrid Mesh I and original polygonal elements have similar accuracy for the errors of lower and upper edges of the gap where the Hybrid Mesh II give the lowest accuracy for the lower edge of the gap.

Table 4.6 Comparison errors of band gap ranges in TM mode of a square lattice unit cell for hybrid polygonal FEM

Mesh	Error of lower edge of the gap (%)	Error of upper edge of the gap (%)	Error of band gap ranges (%)	Ratio of the predicted width of band gap with PWEM
Hybrid Mesh I	1.47187	1.28465	0.78197	100,78%
Hybrid Mesh II	2.06922	1.29559	0.78170	99,22%
Polygonal Mesh	1.67237	1.28678	0.25142	100,25%

In order to convince this analysis, Figure 4.15 presents the accuracy of the band gap characteristic of the square lattice PC related to the variation of the r/a ratio using polygonal FEM whose n>3 elements in uniform meshes with almost the same number of unknowns. The graph indicates that the larger diameter of the dielectric rod gives the larger approximation errors where the fluctuating area decreases and the non-fluctuating area increases. It means that the performance of the higher order elements on that high dynamic area is more reduced while the enlarging non-dynamic area needs more h-refinement inside so that due the enlarging lower accuracy area, the accuracy is reducing as indicated in the Figure 4.15.

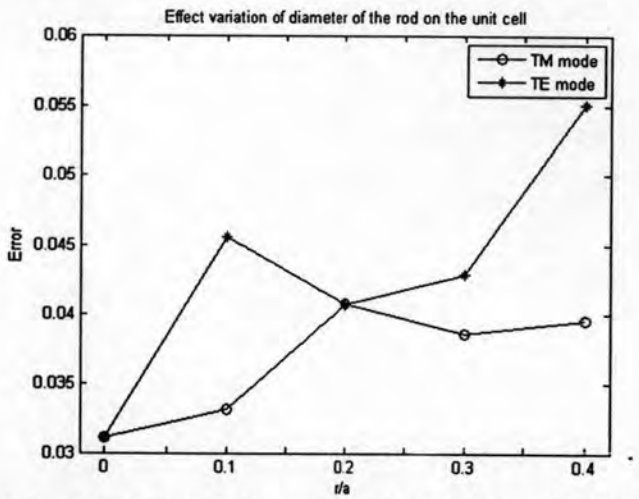

Figure 4.15 Variation effect of r/a in the accuracy of the band gap characteristic using polygonal FEM.

4.6 Convergence rate testing of polygonal FEM

After all investigations of the characteristic of the polygonal FEM on the unit cells, here the convergence rate graphs are presented. The polygonal elements used to observe the convergence rate are available in Appendix B. The convergence rate tests are taken for both TM and TE modes using some cases of meshes given in Figure 4.16 that yield those graphs shown in Figure 4.17. Case I is the linear triangular FEM. Case II represents the polygonal FEM while the Case III yields the hybrid polygonal FEM. In

order to test the convergence rate that need large number of unknowns to investigate, the higher order elements are represented by n=4 elements.

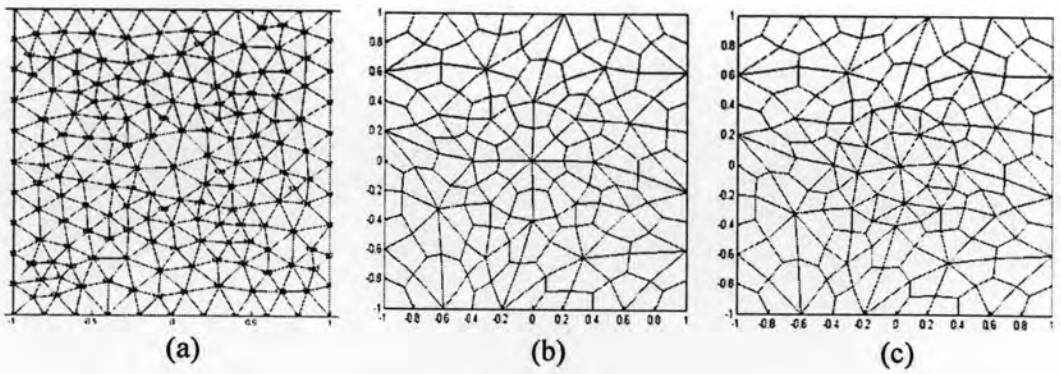

Figure 4.16 Types of meshes for (a) case I, (b) case II, and (c) case III.

The convergence rate graphs for case II and case III are fluctuating significantly with the increased number of unknowns. Considering the source design of the meshes, this condition can be reasonable. Increasing number of unknowns must consider about the behavior of the field on the analyzed domain. In polygonal FEM as well as in common other common FEM, elements on the dynamic areas must be refined more than the non-dynamic ones. The part of the domain where the mode is concentrated should be refined more than the others should. Improper refinement might make the accuracy low. The designed meshes for these fluctuating error ranges can be seen in the appendix B based on the number of unknowns (nodes).

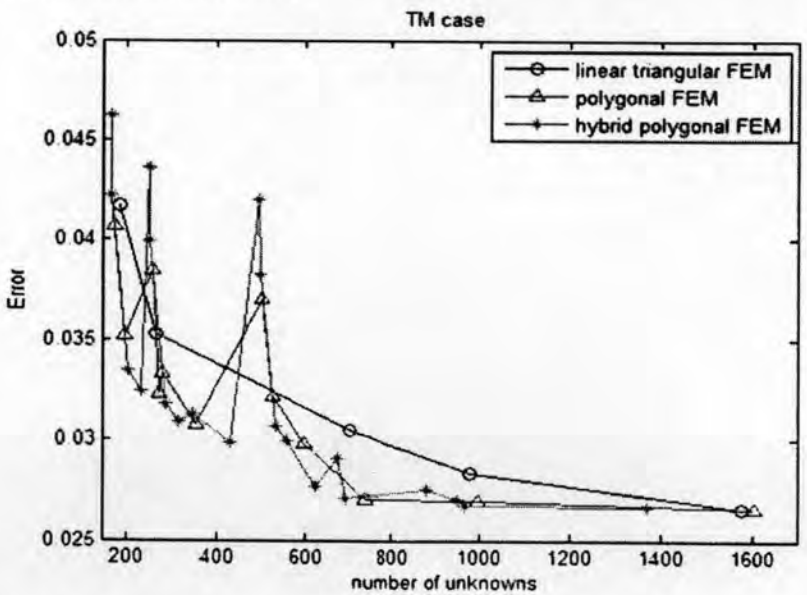

Figure 4.17 Convergence rate test for all polygonal mesh in Appendix B (B.1) for TM and TE modes

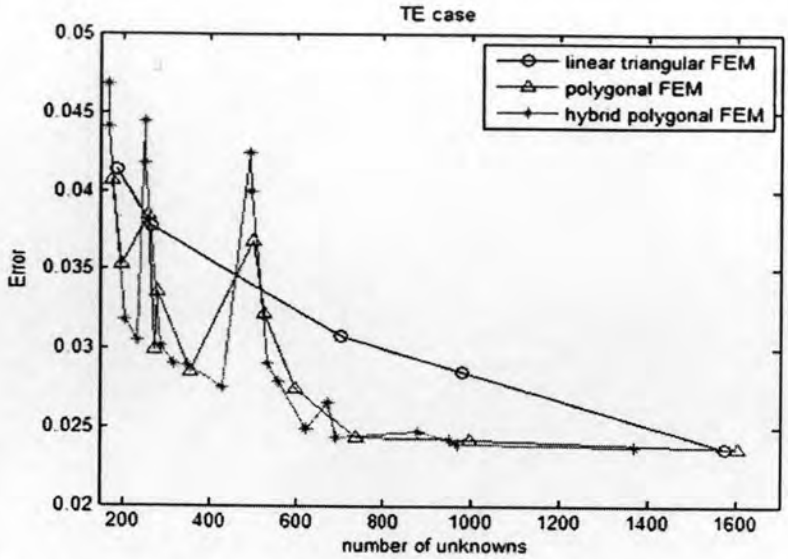

Figure 4.17 Convergence rate test for all polygonal mesh in Appendix B (B.1) for TM and TE modes (cont.)

Here are some examples of the meshes from Case II and Case III which will raise the error though the number of nodes is increased compared to which that give the better accuracies with comparable number of unknowns.

For case II:

Polygonmesh6: Number of nodes = 355 Number of elements = 334 error_tm = 0.03072 error_te = 0.02844 BETTER	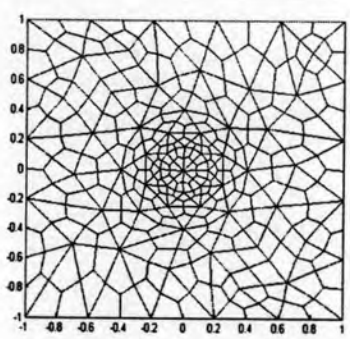
Polygonmesh7: Number of nodes = 503 Number of elements = 478 error_tm = 0.03702 error_te = 0.03683 WORSE	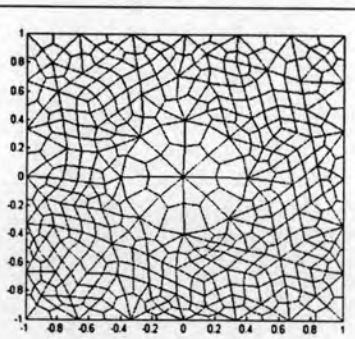

Since the unit cell used here is in case of rod embedded in air medium, the fields are more concentrated in the rod. The rod here is modeled by the circle at the center of the unit cell.

The two polygonal meshes above show the different type of refinement in case of increasing the number of unknowns. The second mesh refines the air medium more than the rod such that the number of unknowns in the rod is reducing. The results show that the average approximation error increases although the number of unknowns has been raised. The errors of the results increase around 25 % while the number of unknowns become 41,7 % larger. The case III will face this problem as well as seen in the examples.

For case III:

Mixmesh 4 Number of nodes = 234 Number of elements = 294 error_tm = 0.03243 error_te = 0.03047 BETTER	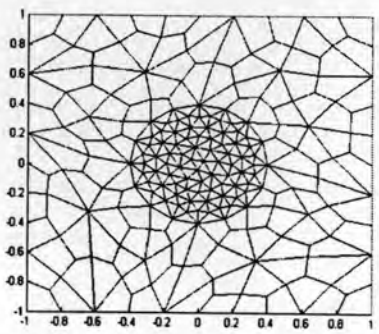
Mixmesh5 Number of nodes = 251 Number of elements = 246 error_tm = 0.04358 error_te = 0.04447 WORSE	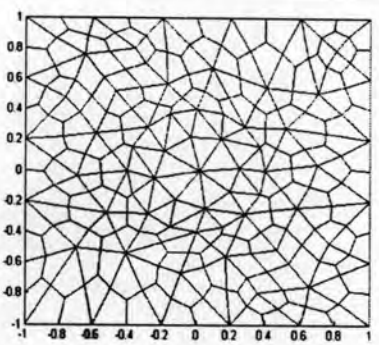

The same analysis is taken for the results of the comparison in case III. Increasing the number of unknowns only 7,2 % can increase the errors until 40,2 %. The little refinement occurs in the air medium while the nodes in the rod become less in the number. This condition has been shown in case II that uses all higher order elements. However, the case III employs the lower order elements to approximate the fields in the rod. Therefore, reducing the number of unknowns in the rod from lower order elements would make the accuracy much worse than case II where the elements are higher order. This makes the case III become more sensitive. When the mesh is not designed properly, the error could raise sharply.

From the previous results (sub-chapter 4.3.1), the modification of the mesh from polygonal elements to the hybrid/mixed types of elements give a higher accuracy where the number of triangles in the rod are equal to the number of sub-triangles of polygonal elements in the rod. So, it might be concluded that in order to get a better accuracy from Case II, the number of triangles inside the rod for Case III must be at least equal to or

larger than the number of sub-triangles of polygonal elements in Case II which are used for numerical integration.

Therefore, some designed meshes in the previous ones must be smoothed in order to get the better convergence rate graphs as shown in Figure 4.18 - 4.19.

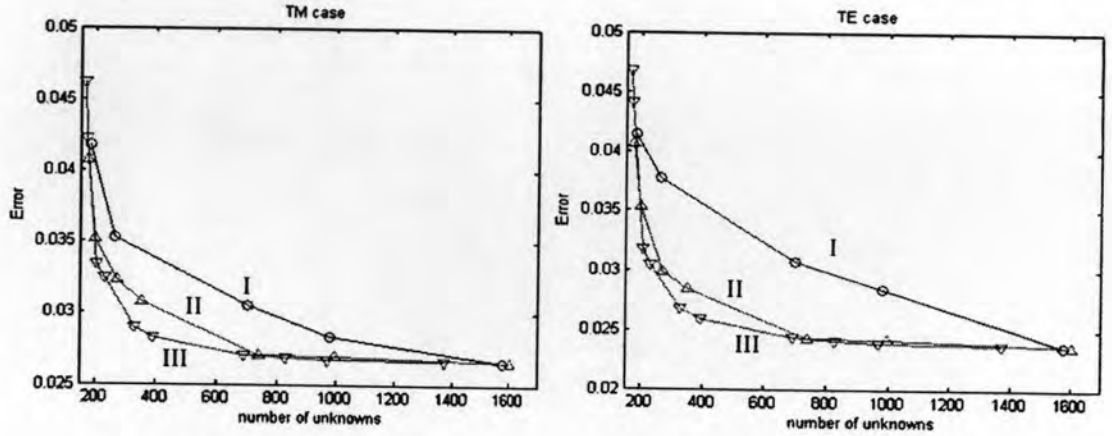

Figure 4.18 Convergence rate test for all polygonal meshes related to the number of unknowns for TM and TE modes

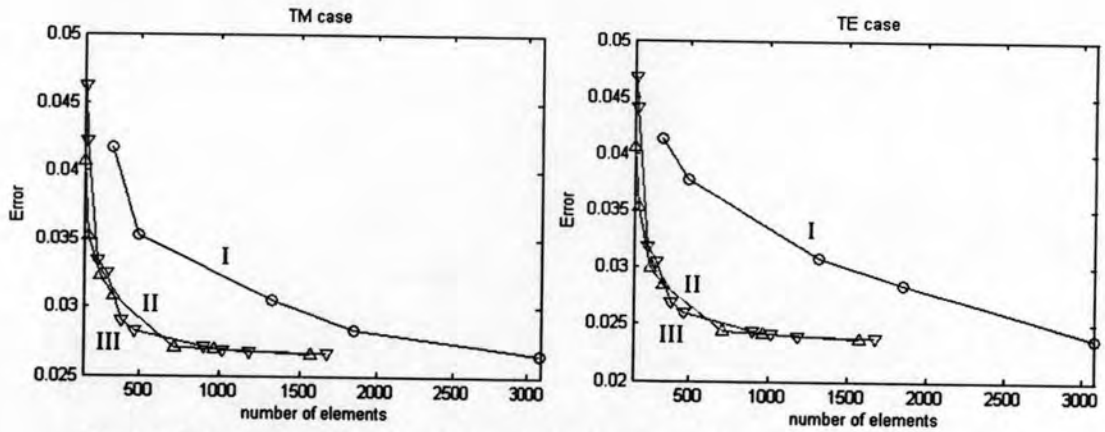

Figure 4.19 Convergence rate test for all polygonal meshes related to the number of elements for TM and TE modes

As the number of unknowns increases, the convergence rate for Case I, II and III finally yield the same level of error. The convergence rate test shows that the polygonal FEM with a polygonal mesh of all n>3 elements will give a quick step to converge than the linear triangular FEM until around 1000 numbers of unknowns. More than 1000 number of unknowns, the convergence rate graphs tend to converged to a particular value of error. The efficiency of the method looks more significantly in terms of the number of elements as in Figure 4.19. The convergence rate in term of the average error is useful to select the best meshes with the lowest average error of the solutions.

Increasing the number of nodes using the polygonal mesh is quite sensitive in the accuracy. The behavior of the system must be understood well so that the assigned higher order polygonal elements or the linear polygonal elements can be optimum for the accuracy.

In order to investigate the main property of the band gap characteristic, i.e. the frequency band gap, the convergence rate resting around the available band gap should be considered. The Figure 4.20 and Figure 4.21 show the tendency of the approximate solutions of the polygonal FEM related to the reference solutions for the lower and the upper frequency gap, respectively. The comparative results are given from the linear triangular FEM and hybrid polygonal FEM.

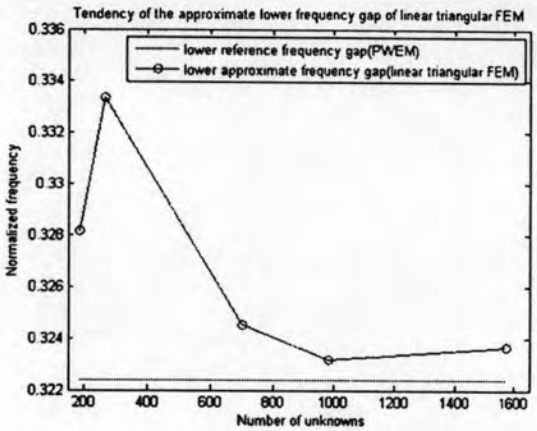

(a) Av.error: 1.76094%

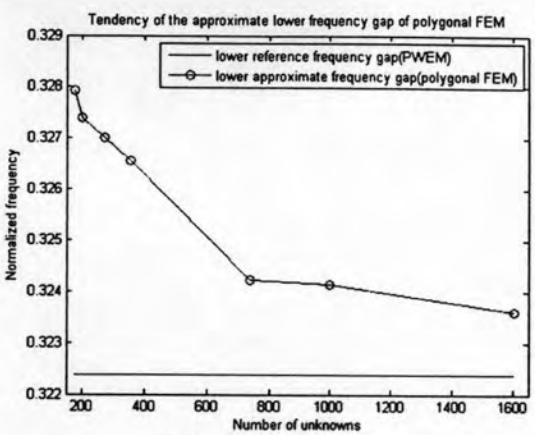

(b) Av.error:1.28575%

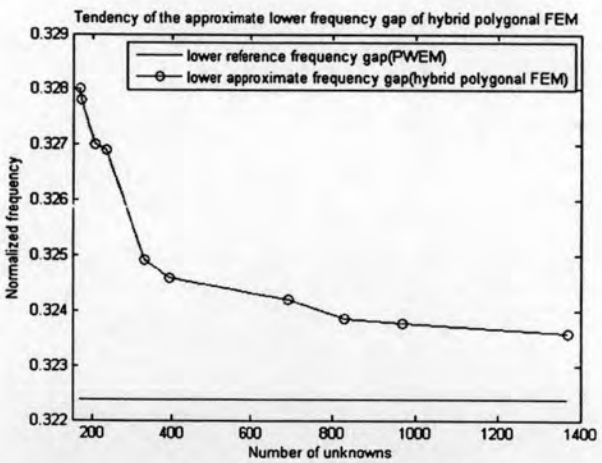

(c) Av.error:1.08657%

Figure 4.20 Tendency of the approximate lower frequency gap of (a) case I, (b) case II, and (c) case III.

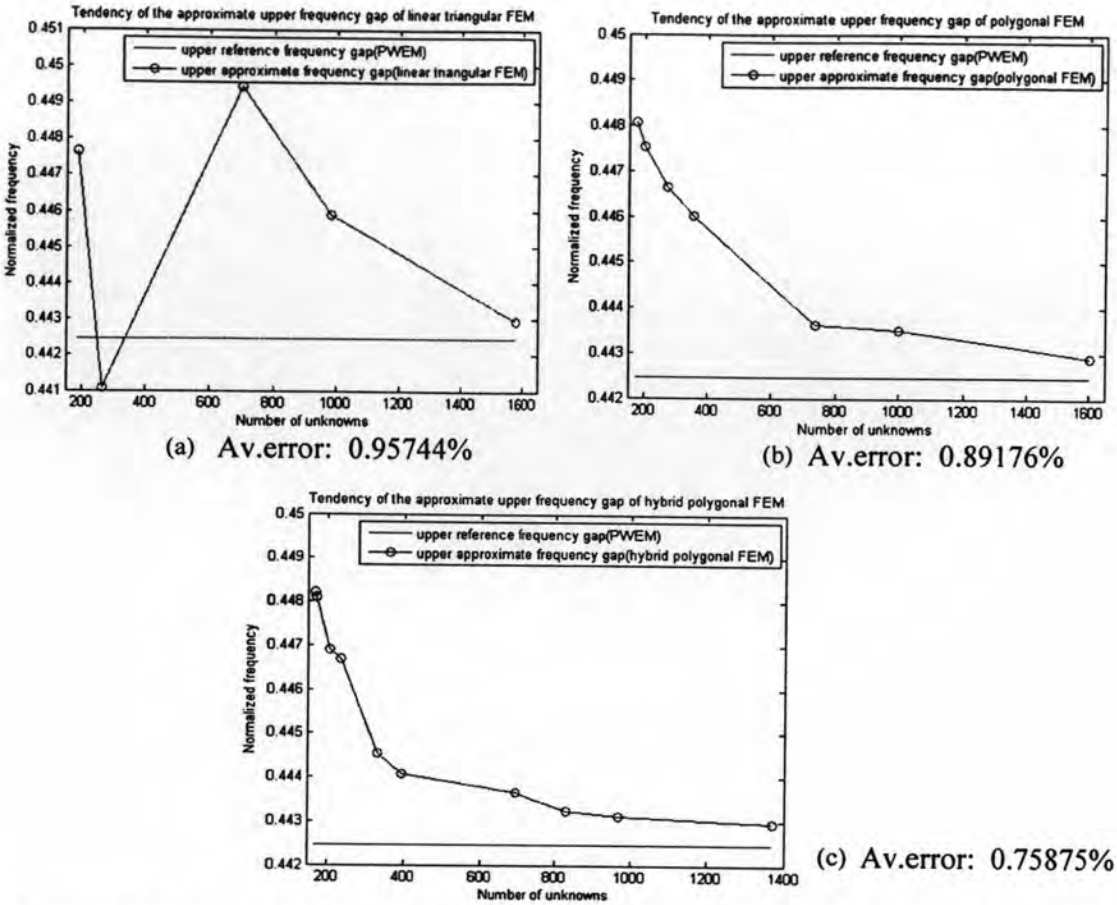

Figure 4.21 Tendency of the approximate upper frequency gap of (a) case I, (b) case II, and (c) case III.

From both figures above, the results from linear triangular FEM show high oscillation that give the highest average error from the plotted values while the polygonal and the hybrid polygonal FEM give graphs that are more convincing to converge.

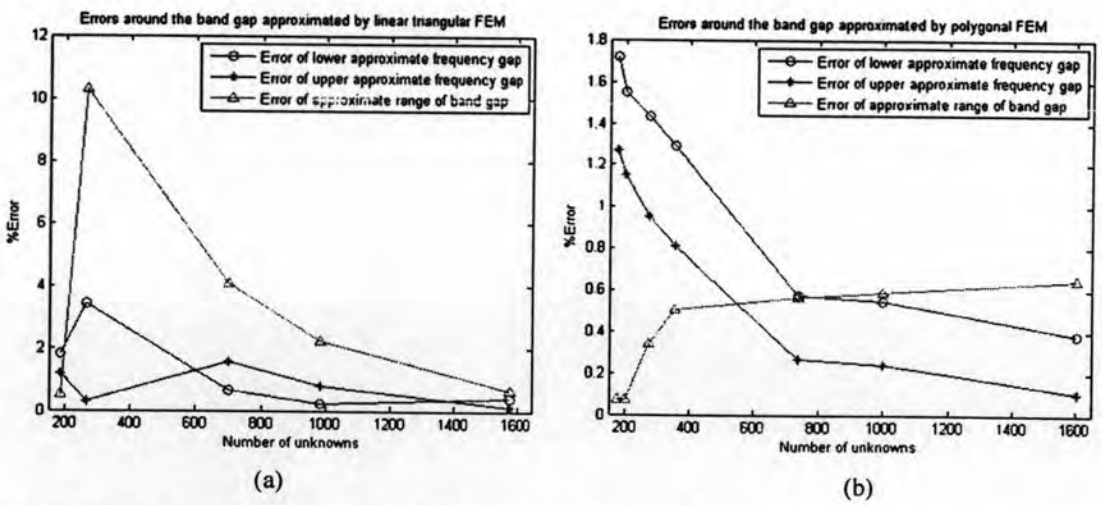

Figure 4.22 Percentage errors around the approximate band gap of (a) case I, (b) case II, and (c) case III.

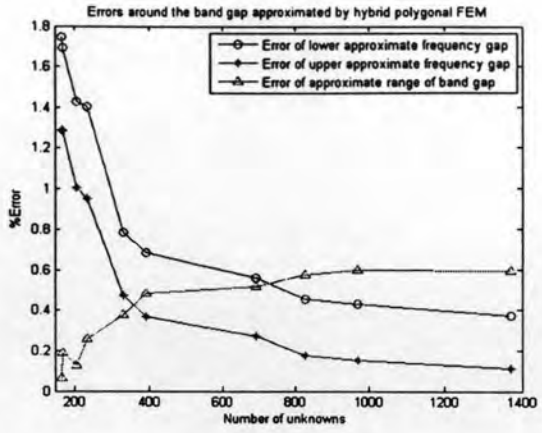

(c)

Figure 4.22 Percentage errors around the approximate band gap of (a) case I, (b) case II, and (c) case III (cont.)

The percentage error graphs in Figure 4.22 show that the results of polygonal FEM converge quickly than the linear triangular FEM. Using around 300 numbers of unknowns (nodes), the upper and lower frequency of the gap are approximated by less than 1% error while the linear triangular FEM needs around 1000 nodes for them to reach less than 1% error. This comparative result proves that the efficiency of the polygonal FEM is more than the linear triangular FEM. The related graphs are presented in blue lines.

The red lines show the related percentage error of the frequency band gap. In this case, the tendency of the red lines for both polygonal FEM and the hybrid FEM is asymptotic to around 0.6 % error as well as the linear triangular FEM. However, the linear triangular FEM presents the highest peak of the band gap error until 10 % while the other two methods starts from almost 0% error. The saturated error of the polygonal and hybrid polygonal FEM for the band gap range occurs because the upper frequencies of the gap converge faster than the lower ones as shown in Figure 4.23.

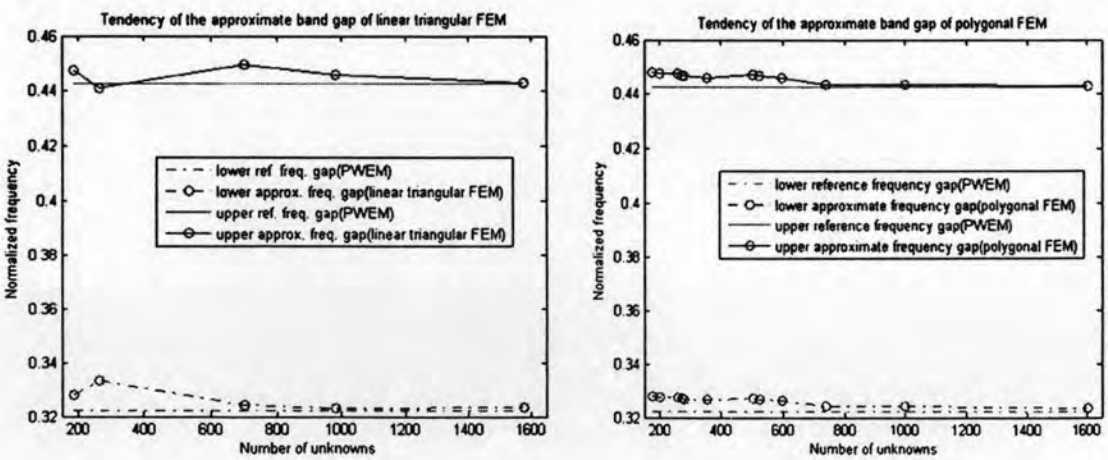

(a) (b)

Figure 4.23 Tendency of the approximate band gap of (a) case I, (b) case II, and (c) case III

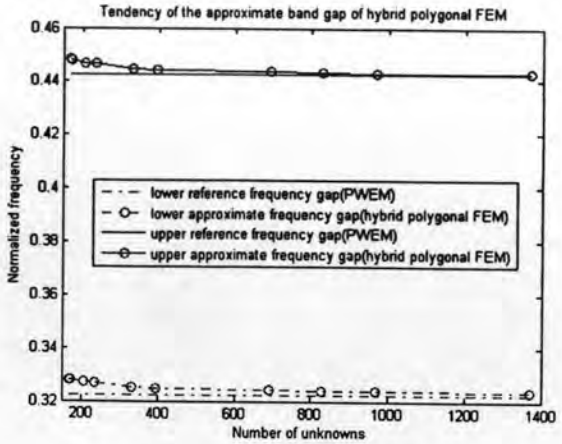

(c)

Figure 4.23 Tendency of the approximate band gap of (a) case I, (b) case II, and (c) case III (cont.)

Figure 4.23 shows that the values of the upper frequency gap from polygonal FEM converges sufficiently with 700 nodes while the linear triangular FEM needs 1600 nodes to obtain the same value. In this case, the higher order polygonal meshes are built from n=4 elements for early investigation of the performance of Wachspress shape function. The limitation of the order of polynomials obtained by n=4 elements may cause this saturated condition of the approximation values especially for the lower frequency of the gap. The accumulated discretization errors increase as well as the linear triangulation.

As a consideration, Figure 4.6d with 263 nodes with dominant n>5 elements provide error as follow:

Polygonal mesh of dominant n>4 dominant elements with 263 number of unknowns	Error lower frequency of the gap :	1.45012 %
	Error upper frequency of the gap:	0.61090 %
	Error of the band gap range:	1.64249 %

Based on this result, when the convergence rate is built by higher order elements with n>4, better solution can be predicted to obtain. It can be compared when the n=4 elements are used with almost equal number of unknowns. The related errors are as follows.

Polygonal mesh of dominant n=4 elements with 273 number of unknowns	Error lower frequency of the gap :	1.43192 %
	Error upper frequency of the gap:	0.95089 %
	Error of the band gap range:	0.34075 %

The above comparison shows that the upper approximated frequency of the gap is more converged by using higher order elements as well as the lower approximated frequency of the gap although the upper one is more converged than the lower one. The upper frequency of the band that has a higher frequency looks more appropriate to be approximated using the higher order interpolation functions rather than the lower

frequency of the band where the accuracy of the lower frequency one does not increase significantly. This behavior is also presented in Figure 4.22b-c of the polygonal FEM and the hybrid polygonal FEM where the upper frequency of the band is more converged than the lower frequency of the gap. In contradiction, the graph in Figure 4.22a which is obtained from linear triangular FEM has a significant part where the lower frequency of the gap is more converged than the upper frequency one. Though it still needs to be observed more, this part indicates that the linear triangular elements somehow are better to approximate the lower frequency of the gap. It means that with the proper linear triangular mesh, approximation of the lower frequency solution would be enough.

Figure 4.24 shows the computation time when a significant time difference occurs for high number of nodes that proves that the polygonal FEM is faster. Improving the code using an iterative method to solve the eigenvalues can give faster calculation time that is not yet applied in this work. Figure 4.25 shows that the width ratio of the approximated band gap relative to the reference band gap is close to 100% by using the polygonal FEM while the linear triangular FEM gives fluctuating results that can be very far from 100 %, e.g. until around 90%. Comparing to the work in [35] that provide 65 % of this value, this work gives better results in order to approximate the frequency band gap.

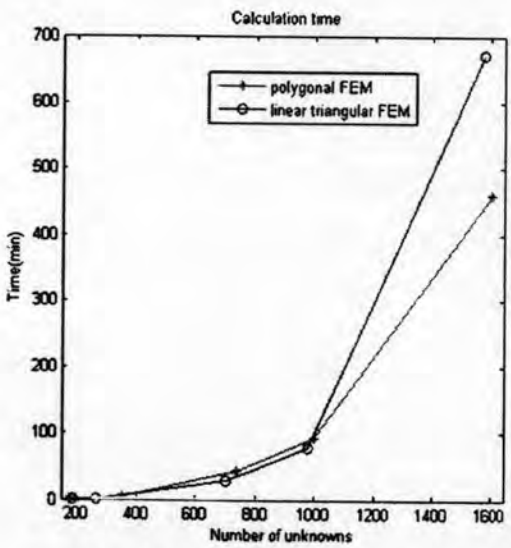

Figure 4.24 Size of unknown vs. computation time

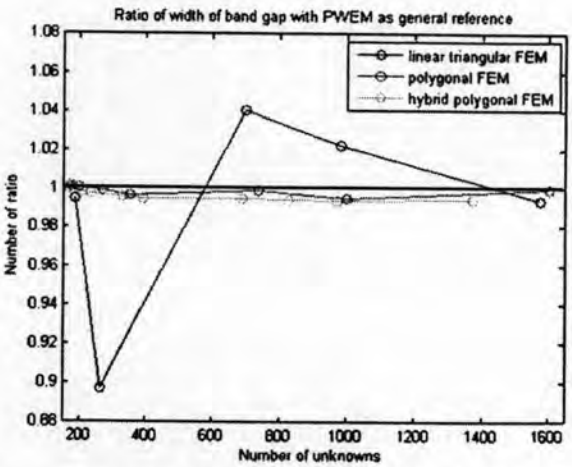

Figure 4.25 Ratio of the width of the band gap

4.7 Applications on non-ideal 2D PCs

4.7.1 Cracked rod in the unit cell

The possibility of the crack happen onto the 2D photonic crystals has been studied recently in [36]. The crack happened due to the defect in fabrication process instead the deformation of the geometry of the structures. The paper mentioned that a chemical assembly to produce the ZnO PCs, which is a simpler and less costly approach to generating large-scale PCs than lithography does. This self assembly method might lead the existing crack because of unbalanced evaporation temperatures and crystal growths,

where these two factors are the most importance ones for crystalline quality. This method is useful to fabricate thin polystyrene PCs in water in order to investigate emission from dye-incorporated PCs [22]. The good crystalline quality needs the compromise between a higher evaporation temperature and a slower crystal growth rate. The higher evaporation temperatures will make the material spheres to have the more kinetic energy to explore possible lattice sites, so the defects such as vacancies, dislocations, and also cracks are reduced. However, when the evaporation temperature is too high, the evaporation rate become faster which means that the crystal growth rate is higher as well. Faster growth rate leads more defects in the structure [36]. The paper concluded that the ability to control crack formation in PC might open possibilities of producing simple and inexpensive microcavities or waveguides between PC mirrors in which the nature of the light in cracks is not clear at the present time [36]. For this case, an appropriate numerical tool might be used to analyze such cracked structures. Here, the performance of the FEM formulation is investigated to analyze un-ideal structures of 2D PCs. In [36], it is stated that the photoluminescence emission spectra depended on the PC domain size and on the concentration of cracks.

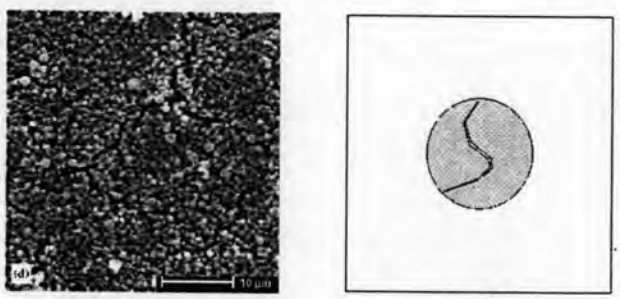

(a) (b)

Figure 4.26 (a) A real cracked PC structure [35] and (b) model of a cracked rod of a square lattice unit cell

Figure 4.26 gives an example of a cracked structure of such PC in [36] and a created model of a cracked rod of a square unit cell with dielectric constant of the rod is 8.9. With the condition of the cracked geometry, the band gap characteristic is analyzed and will be compared with the ideal rod on the unit cell. The comparison is taken by running the analysis using two methods, which are the linear triangular FEM and the polygonal FEM as the meshes are shown in Figure 4.27.

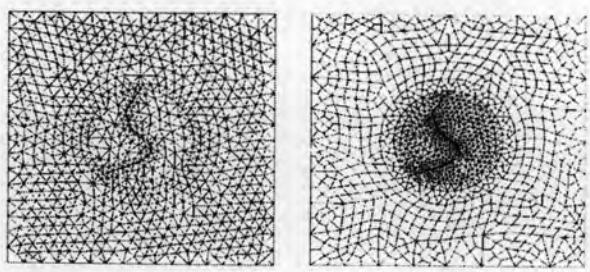

(a) (b)

Figure 4.27 Models of analyzed designs of a cracked rod on a square unit cell using (a) a linear triangular mesh (Mesh A) (b) hybrid polygonal meshes

Analyzing the cracked rod of the square lattice PCs on one unit cell will give an assumption that all unit cells constructing the 2D PCs have the same structure of the rods infinitely as shown in Figure 4.28 below.

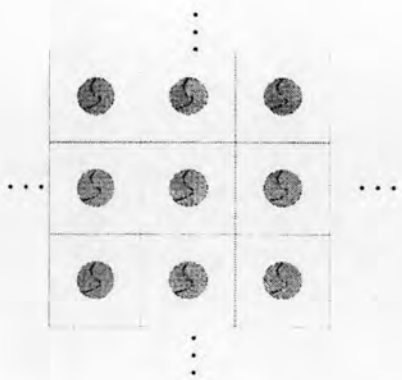

Figure 4.28 The arrangement of unit cells of a infinite square lattice PC with cracked rods

The cracked rod is modeled by inserting the rod using the air gap that fills 1.068 % of the rod. Because the unit cell is periodic, it is assumed that all the unit cells have the same geometry structure infinitely. The related band gap characteristics obtained from two meshes are shown in Figure 4.29 while the related errors are given by Table 4.7.

Table 4.7 Comparison errors of linear triangular FEM and hybrid polygonal FEM for a square unit cell with a cracked rod

Mesh	Linear triangular FEM (Mesh A)	Hybrid polygonal FEM
Av. Error TM	0.02839	0.02762
Av. Error TE	0.03291	0.03145

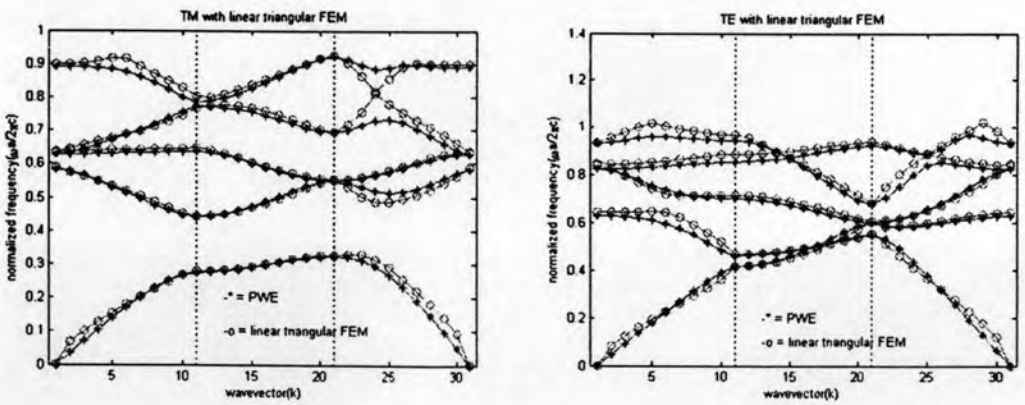

(a)

Figure 4.29 Results of band gap characteristics of a cracked rod model with air gap fill 1.068 % of the rod from (a) Mesh A and (b) Hybrid polygonal mesh

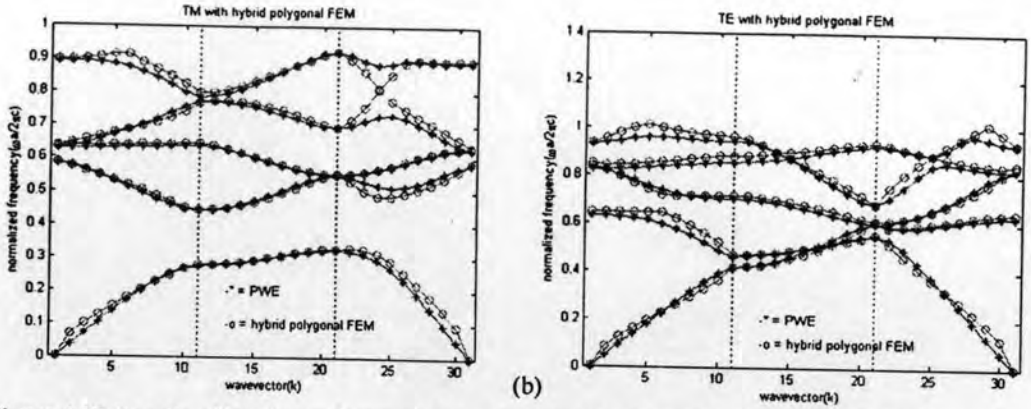

(b)

Figure 4.29 Results of band gap characteristics of a cracked rod model with air gap fill 1.068 % of the rod from (a) Mesh A and (b) Hybrid polygonal mesh (cont.)

From the Figure 4.28 and the Table 4.7, the existing crack inside the rod does not give any significant effect yet to the accuracy of the band gap characteristics. For the investigation, the linear triangular FEM is employed first to see the behavior of the cracked structures.

When the area of the crack is widened, the assumption of the structure now is shown in Figure 4.30 with air gap fill 2.362 % of the rod while Figure 4.31 shows its band gap characteristics.

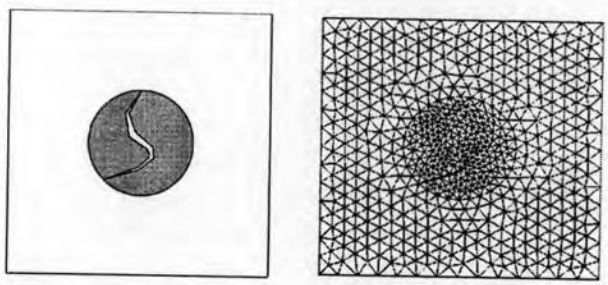

Figure 4.30 A cracked rod model with air gap fill 2.362 % of the rod with its triangulation (Mesh B).

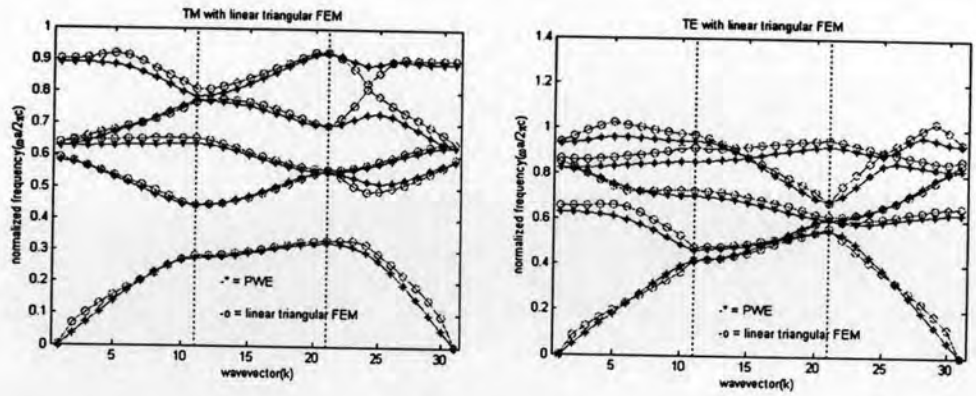

Figure 4.31 Results of band gap characteristics of a cracked rod model with air gap fill 2.362 % of the rod.

When the crack is over the boundary, there is continuity between the rod and the medium as shown in Figure 4.32 where the air gap is 2.95 % of the rod. Figure 4.33 presents the created band gap characteristics.

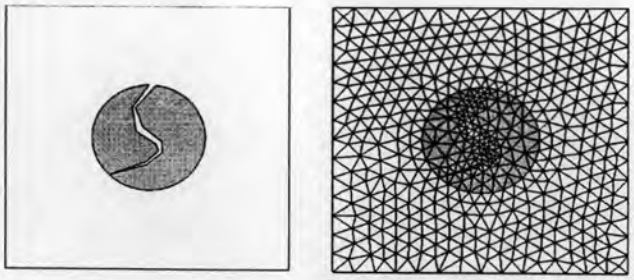

Figure 4.32 A cracked rod model with air gap fill 2.95 % of the rod with its triangulation (Mesh C).

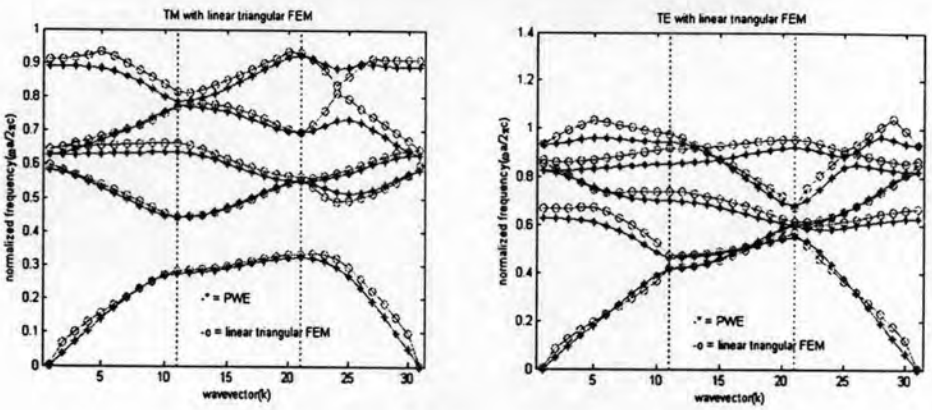

Figure 4.33 Results of band gap characteristics of a cracked rod model with air gap fill 2.95 % of the rod

The distorted geometries of the rod so far do not make any significant change to the band gap characteristic. When the crack passes through the boundary, the change of the dispersion relation indicates to increase. Another example is given in Figure 4.34 when the crack passing through the boundary is enlarged so that the air gap is 7.57 % in the rod the almost significant change of the band gap characteristics are shown in Figure 4.35.

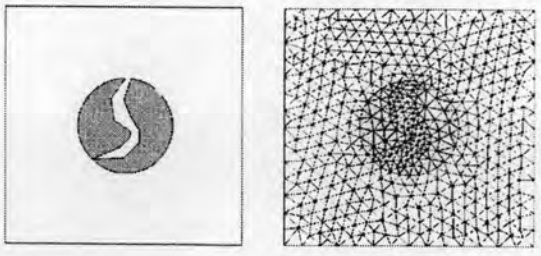

Figure 4.34 A cracked rod model with air gap fill 7.57 % of the rod with its triangulation (Mesh D).

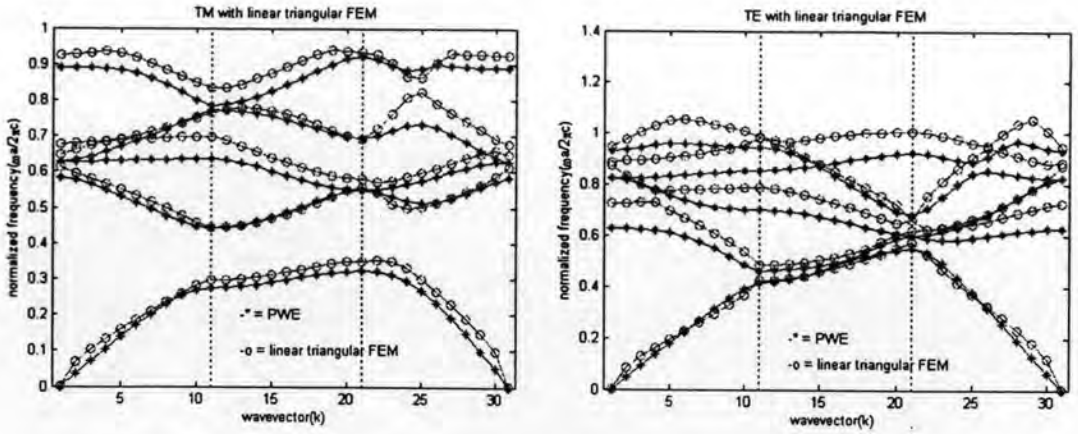

Figure 4.35 Results of band gap characteristics of a cracked rod model with air gap fill 7.57 % of the rod

The last distortion of the geometry gives an effect where the values of eigenfrequencies tend to be higher. It makes sense because the larger portion of air gap in the rod creating the crack decreases the volume of the dielectric material. This also reduces the filling factor. In this case, the concentration of the lower frequency band used to stay in the higher dielectric materials is reduced as well so that the bands are forced to raise the frequencies. Though the accuracy might not high enough, the tendency of the changing of the band gap characteristic can be seen. This condition agrees with other works [35]. For all results obtained by linear triangular mesh, the related average errors are given in Table 4.8 where the larger crack raises the error due to the raising frequencies with almost similar numbers of unknown especially for Mesh C and Mesh D.

Table 4.8 Comparison errors of cracked models of unit cells

Mesh	Mesh A	Mesh B	Mesh C	Mesh D
Number of nodes	805	655	500	515
Number of elements	1544	1252	942	972
Av. Error TM	0.02839	0.03095	0.03513	0.05447
Av. Error TE	0.03291	0.04311	0.04882	0.08379

The information of the band structure in [36] was obtained by performing transmission measurements by changing the angle of incidence onto one sample of cracked structure. The band gaps found from the measurements were broad and deep. The observed band gaps were almost independent of the density of cracks while this research shows numerically that the higher volume of crack leads the frequency bands as well as the band gaps moving to the higher frequency region as given in Figure 4.35. However, this research also observes that when the difference of the crack volume is not significant (relative small), the band gap characteristics look unchanged as shown in Figure 4.29 and Figure 4.31.

However, the density of the cracks and the domain size of the structure proved to affect the photoluminescence (PL) emission spectra. In [36], for structures consisting of large domains and low density of cracks (small crack volume in the structure), the PL emission exhibited a single peak while in small domains and high density of crack (large crack volume in the structure), the double-peak PL emission occurred where the blue shifted emission was recognized. The light channeling within the crack showed unsmoothed modes as in [36]. Here, the existing modes of the crack are shown in Appendix C where the light channeling within the crack can be recognized clearly in TE modes (*H*-polarization).

4.7.2 Deformation of the rod in the unit cell

Another possibility of an un-ideal structure in the PCs is the deformation of the geometry of the structure that leads non-ideal form of the rods because of the imperfect fabrication process. A model of a square unit cell with disordered geometry of the rod is shown in Figure 4.36 including its meshes using linear triangular elements and higher order polygonal elements. This model is taken by considering the work of [37] in its application to photonic crystal fibers (PCFs) where the distorted rod becomes 188,37 % of the ideal rod.

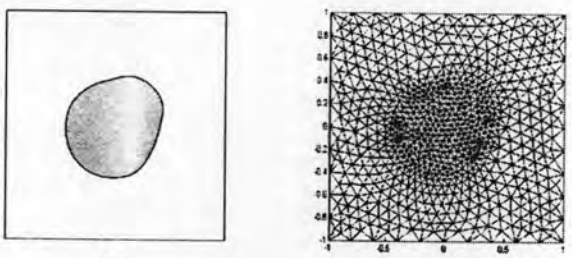

(a) (b)

Figure 4.36 (a) model of a square unit cell with a deformation on the rod, (b) the mesh using linear triangular elements

By taking the analysis over one unit cell, the configuration of the system can be interpreted as in Figure 4.37 where all unit cells of the PC will have the same geometry as such one unit cell. Figure 4.38 shows the results of the band gap characteristic of the unit cell in Figure 4.36.

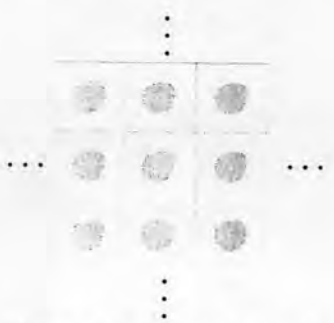

Figure 4.37 The arrangement of unit cells of a infinite square lattice PC with deformation in the rod

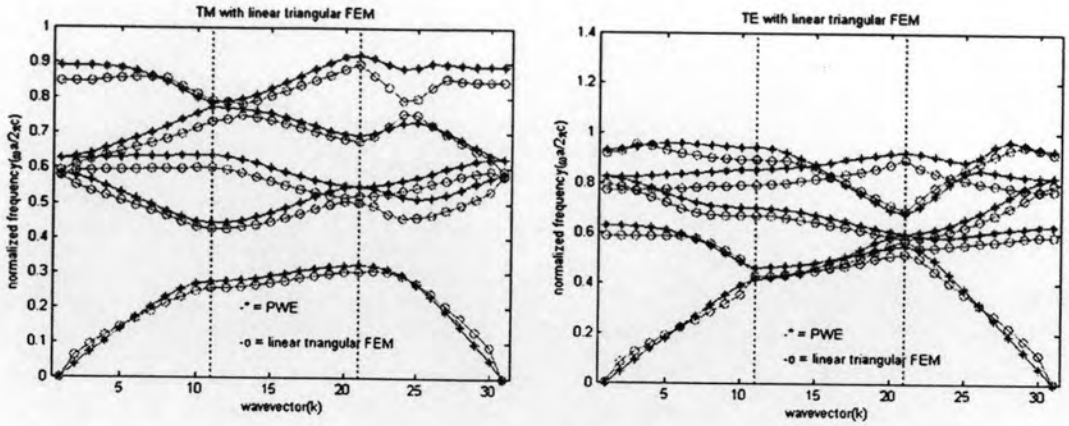

Figure 4.38 Band gap characteristics of the model of deformed rod.

Table 4.9 Resulted error of the deformed rod

Mesh	Linear triangular mesh
Error TM	0.05086
Error TE	0.05255

From the recent results, the deformation of the geometry of the structure gives effect more significantly compared to which from the cracked geometry. The deformation of the rod forces the bands to decrease their frequency where also affect to the range of the band gap. In the TM mode solution, another thin band gap exists in the higher frequency range between band 5 and band 6. The results of the eigen-frequencies tend to move to the lower values compared to reference results.